

A review on interferometry lightning mapping system and its deployment in Palembang Indonesia

Wiwin A. Oktaviani^{1,2}, Muhammad Abu Bakar Sidik³, Mohd Riduan Ahmad⁴, Muhammad Irfan Jambak³

¹Doctoral Student in Engineering Sciences, Faculty of Engineering, Universitas Sriwijaya, Palembang, Indonesia

²Department of Electrical Engineering, Faculty of Engineering, Muhammadiyah University of Palembang, Palembang, Indonesia

³Department of Electrical Engineering, Faculty of Engineering, Universitas Sriwijaya, Indralaya, Indonesia

⁴Centre of Technology for Disaster Risk Reduction (CDR), Fakulti Teknologi dan Kejuruteraan Elektronik dan Komputer (FTKEK), Universiti Teknikal Malaysia Melaka (UTeM), Melaka, Malaysia

Article Info

Article history:

Received Jul 28, 2023

Revised Aug 15, 2024

Accepted Aug 25, 2024

Keywords:

Climate change

Interferometry

Lightning activity

Lightning detection system

Lightning protection system

Renewable energy

ABSTRACT

Climate change effects influence the sustainability of wind and photovoltaic energies as renewable sources. Similarly, infrastructure for renewable energy is structurally vulnerable to lightning strikes. Hence, a system for detecting and monitoring lightning activity is necessary to predict and adapt to climate change trends and to enhance the lightning protection system's capability. One such system for observing and locating lightning is very high frequency (VHF) interferometry. Various factors, such as the baseline distance between sensors, the frequencies used, and the quality of the analyzed signal, will influence the system's accuracy. This paper discusses these factors through an extensive literature review. This study aims to identify the factor that most significantly affects the system's accuracy and to determine the technical adjustments required to improve this accuracy. Enhanced precision in the interferometry system will provide a more detailed view of lightning activity, thereby aiding in the climate change prediction that could impact electricity generation from renewable sources. Accurate lightning location detection can also serve as a basis for designing effective lightning protection systems for renewable energy infrastructure.

This is an open access article under the [CC BY-SA license](#).



Corresponding Author:

Muhammad Abu Bakar Sidik

Department of Electrical Engineering, Faculty of Engineering, Universitas Sriwijaya

Jalan Raya Palembang-Prabumulih Km. 32, Indralaya, Kabupaten Ogan Ilir, South Sumatra, Indonesia

Email: abubakar@unsri.ac.id

1. INTRODUCTION

The production of energy from wind turbines and photovoltaic systems requires high initial investment; thus, the goal is to generate as much energy as possible to recoup these costs. In contrast to fossil fuels, energy from renewable sources is intermittent since weather and climatic factors impact the energy supply. The resilience and sustainability of renewable energy sources (wind and PV) may be threatened by climate change with extreme and violent weather occurrences [1]. Therefore, these systems must be designed to withstand weather variability, considering the impacts of climate change [2].

Large-scale atmospheric circulation pattern changes that significantly modulate temperature and wind, altering energy production from wind generation and leading to natural climate change [1]. For example, with increasing temperature, the maximum decrease in wind power generation in the US is 0.6%-1.0% in the mid-century and 0.8%-1.9% at the end of this century [3]. Solar energy is also impacted by climate change. This condition is brought on by changes in the permeability of the atmosphere due to

variations in humidity, turbidity, and cloud features, which affect solar radiation and the ability of photovoltaic panels to generate power [4].

Numerous studies [5]-[12] have demonstrated a strong correlation between lightning and climate change. Holzworth *et al.* [13] indicated a significant increase of 800% in lightning activity in the Arctic region over a decade (2010-2020). Holzworth *et al.* [13] also stated that with a global temperature anomaly increase of 0.5 °C, there would be a 100% increase in the lightning strike rate in the Arctic compared to the rate in 2020. The observations in Antarctica clearly demonstrated climate change. Another study showed that in a warm atmosphere, lightning discharges could produce a substantial amount of nitrogen oxides (NOx), strongly tied to ozone generation and the balance of the earth's radiation [7]. This condition might affect solar panel production.

The International Renewable Energy Agency (IRENA) aims to limit global warming to 2 °C. Therefore energy-related carbon dioxide (CO₂) emissions must reduce by 70% by 2050 [14]. This condition implies that by 2050, solar energy generation must increase by around 22%, and wind energy generation must increase by about 36% [15]. In order to preserve the sustainability and resilience of the renewable energy system, lightning observation and location systems are one of the efforts to observe the trend of climate change patterns that would affect the production of renewable energy.

Indonesia aims to achieve a minimum utilization of renewable energy in the national energy mix of at least 31% by the year 2050 [16], making studies on lightning characteristics essential to support the attainment of this target. However, studies on lightning characteristics associated with climate change have yet to be extensively conducted in Indonesia. The increasing number of incidents of oil refinery facilities catching fire due to the rise in lightning activity in recent years indicates that Indonesia is not immune to global climate change. Despite the presence of lightning protection systems in these vital facilities, such incidents highlight the importance of having lightning observation and localization systems. Monitoring lightning activity will provide engineers with essential information to design improved quality protection systems.

Lightning is a natural phenomenon where lightning involves the movement of charge vertically due to the release of positive or negative charges. This charge release process will produce electromagnetic emissions with the frequency range of very low frequency (VLF) to very high frequency (VHF) [17]. The energy emitted by lightning's electromagnetic emission is so powerful that it can destroy items directly struck by lightning or other objects that encounter electromagnetic wave interference. Thus, to avoid or limit the impact of damage caused by lightning strikes, detecting the lightning position and the direction from which the potential for lightning would hit is required.

Electromagnetic emission is a parameter used to determine the direction of lightning strikes, known as lightning location systems. One of the techniques used in lightning location systems is interferometry, which is the most promising method of determining the location of the strike. It does not require many antennas and sensors and is not susceptible to the noise that usually arises along with the signal to be recorded [18]. In determining the strike's location, the electric field's vertical components are measured using sensors in parallel plate antennas equipped with an electric measuring circuit.

One of the current discussions in the VHF interferometry lightning location system is the accuracy rate of the interferometry technique. Therefore, this article describes factors that may affect the accuracy by reviewing much literature, aiming to provide a better insight into the development. In particular, this article will examine a research question, such as the most critical factor affecting the accuracy of the VHF interferometry lightning location system. This study aims to contribute to this growing area of research by exploring those factors.

Previous research has demonstrated the application of the VHF interferometry system across various geographical regions, including Europe, America, and parts of Asia, notably Japan and China. Inspired by these advancements, we are motivated to adapt and implement this system within Indonesia, with a specific focus on Palembang, South Sumatra. It is our aspiration that the development of this system will significantly enhance the meteorological, climatological, and geophysical observation capabilities currently facilitated by the Meteorological, Climatological, and Geophysical Agency (BMKG), while simultaneously bolstering the growth of renewable energy initiatives in the region of Palembang.

In the initial part of the article, a general understanding of interferometry was presented. The subsequent section delves into the fundamental concepts and determinants of accuracy in interferometry, while the following part highlights recent technological advancements in this field. The paper's remainder outlines the method for measuring electric fields using a parallel plate antenna and constructing a buffer circuit. Finally, the last section of the article comprises a discussion and conclusion.

2. INTERFEROMETRY TECHNIQUE

2.1. Basic principle of interferometry

Lightning discharges radiate strongly at radio frequencies, which may be used to learn about lightning breakdown processes. Interferometric methods may be used to identify the multiple radiation events as a function of time during a discharge and to obtain images of the growing lightning channels inside a

storm, obscured from view at optical wavelengths [19]. Hayenga [20] initiated using the VHF radio interferometry method to study lightning. The researchers in [21], [22] developed this technique with his coworkers to identify the various processes that occur during discharge using a frequency of 34 MHz. Numerous researchers refined and improved the method [23]-[27].

The interferometry technique, in essence, measures the time difference between two pairs of antennas. However, because interferometry operates at VHF frequencies, the distance between antennas is limited to one to five meters, allowing time differences to be measured by calculating phase differences [28]. In other words, the basic principle of interferometry is to estimate phase differences in the various frequency spectrums of a pair of antennas [27]. The phase difference determines the direction of the electromagnetic field emission source. The basic configuration of interferometry technique is presented on Figure 1.

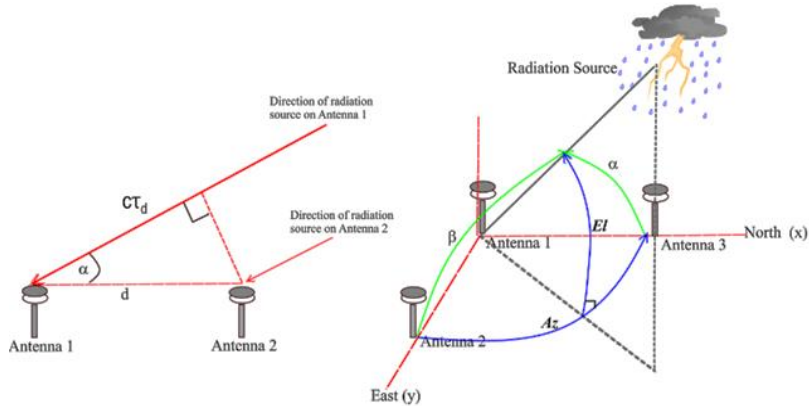


Figure 1. The basic geometry of the interferometry system [18], [29]

The working principle of interferometry technique is as follows; two antennas separated by d meters detect electromagnetic fields emitted by distant sources. This electromagnetic field varies in value to form the sine wave, or cosine wave, with a frequency of ω and wavelength λ . The signal spreads in all directions from the source, and if the distance between the antennas is less than the distance to the signal source, the electromagnetic field is a flat plane. The signal phase as a time function will be different for each location. In other words, because the signal comes from waves coming from different directions, the output signal from two antennas will have a phase difference of ϕ , as shown on Figure 2.

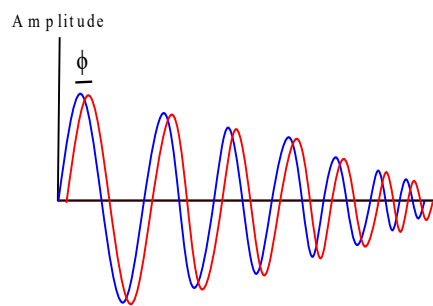


Figure 2. The output signal from two antennas with a phase difference, ϕ [30]

The azimuth and the elevation angles represent the arrival direction. Different phases are denoted as (1):

$$\phi = 2\pi d \sin\theta \cos\varphi / \lambda \quad (1)$$

As previously explained, the measurement of phase difference in interferometry also measures the difference in arrival time at a pair of antennas. From Figure 1, the relationship between arrival time difference τ_d , phase difference $\Delta\phi$ and incident angle α is formulated as (2) [25], [29], [31]:

$$d \cos \alpha = c \cdot \tau_d = \left(\frac{\Delta\phi}{2\pi} \right) \lambda \quad (2)$$

where λ is the wavelength and c is the speed of light.

From (2) it can be calculated the value of the cosine of the incident angle, $\cos \alpha$.

$$\cos \alpha = \frac{c \cdot \tau_d}{d} = \left(\frac{\Delta\phi}{2\pi} \right) \frac{\lambda}{d} \quad (3)$$

The determination of the value of $\cos \alpha$ can be calculated directly from (3) using either τ_d or $\Delta\phi$. The calculation using the phase difference $\Delta\phi$, on the other hand, is slightly more complicated due to the ambiguity of 2π in the phase measurement with baseline $d > \lambda/2$. As described in (1), if $\Theta = \pi/2$ and $d = \lambda/2$ and the value of ϕ is between 0° – 180° , it will cause the phase angle ϕ to vary between 0° – 360° . This condition results in a one-on-one correlation between φ and ϕ . However, if the baseline $d > \lambda/2$, there is a plural value for ϕ , referred to as fringe ambiguity. On the other hand, if d is small enough, the measurement is limited if the antenna distance is quite close. This problem can be overcome by positioning two pairs of antennas with perpendicular baselines of $\lambda/2$ and 4λ [22], [30], [32]. Eventually, this baseline becomes λ and 4.5λ [33]. Shao and Krehbiel [34] employed both short and long baselines in his interferometry system. The problem of fringe ambiguity could be solved by increasing the distance between antennas on the short baseline.

These antennas provide the azimuth and elevation of the sources capable of exciting such an antenna system. Two sets of identical separated antenna can be used to locate the likely position of the lightning source. Table 1 shows the previous antenna distance (baseline) used by some researchers.

Table 1. The interferometry baseline in previous research

No.	Researcher–year	No. of antenna	Baseline
1	Shao <i>et al.</i> –1995 [32]	5	0.5 – 4λ
2	Shao and Krehbiel–1996 [34]	5	0.5 – 4λ
3	Cao <i>et al.</i> –2010 [35]	4	10 m
4	Akita and Kawasaki–2010 [36]	2 stations	10 m
5	Sun <i>et al.</i> –2013 [37]	4	10 m
6	Nakamura <i>et al.</i> –2014 [38]	4	5 m
7	Stock and Krehbiel–2014 [39]	3	10.2 m
8	Wang <i>et al.</i> –2017 [40]	4	18 m
9	Liu <i>et al.</i> –2018 [41]	2 stations	15 m and 16 m
10	Abeywardhana <i>et al.</i> –2018 [42]	4	10 m
11	Puricer <i>et al.</i> –2020 [43]	3	6 m
12	Wang <i>et al.</i> –2020 [44]	7	9 m

The distance between antennas or the baseline must meet the criteria $d/c \geq 1/B$ to obtain this phase measurement [30] where c denotes the speed of light and B denotes the frequency band. However, the value of d will not exceed the transit time $\tau_{transit} = d/c$ between the two antennas, resulting in $\cos \alpha$ of +1. This limit can distinguish between the signal from the actual source and noise [29].

Two additional angles are required to calculate the angle of arrival β relative to the y-axis using calculations based on the horizontal orthogonal baseline. Assuming two baselines in the North and West directions, Figure 1 shows the relationship in spherical trigonometry between incident angle, angle of arrival, azimuth Az, and elevation El.

$$\cos \alpha = \sin(Az) \cos(El) \quad (4)$$

$$\cos \beta = \cos(Az) \cos(El) \quad (5)$$

Geometrically, (4) and (5) transform Cartesian coordinate units to spherical coordinates, where azimuth and elevation are expressed in spherical coordinates as θ and ϕ . At the same time, $\cos \alpha$ and $\cos \beta$ are Cartesian coordinate representations of the x and y axes. The transit time constraint, $\tau_{transit}$, corresponds to $(\cos \alpha)^2 + (\cos \beta)^2 \leq 1$ is a unit radius of the circle in the cosine direction.

In (4) and (5) are derived to obtain the azimuth and elevation using the two arrival times τ_{d1} and τ_{d2} as (6) [29], [31], [45].

$$Az(\theta) = \tan^{-1} \left(\frac{\tau_{d1}}{\tau_{d2}} \right) \quad (6)$$

$$El(\phi) = \cos^{-1} \left(\frac{c}{d} \sqrt{\tau_{d1}^2 + \tau_{d2}^2} \right) \quad (7)$$

In (6) and (7) the azimuth angle is defined to increase clockwise from the North, and the elevation angle increases from the horizon line [31]. For baselines that are not perpendicular to each other, (6) is reduced to (8) and (7) becomes (9),

$$Az = Az_1 + \tan^{-1} \left(\frac{\tau_{d1} \cos(\Delta\theta) - \tau_{d2}}{\tau_{d1} \sin(\Delta\theta)} \right) \quad (8)$$

$$El = \cos^{-1} \left(\frac{c}{d} \sqrt{\frac{\tau_{d1}^2 + \tau_{d2}^2 - 2\tau_{d1}\tau_{d2} \cos(\Delta\theta)}{\sin^2(\Delta\theta)}} \right) \quad (9)$$

where Az_1 is the azimuth of baseline 1, $\Delta\theta$ is the azimuth difference between baseline 1 dan baseline 2 (Az_2), and the angle between the two baselines.

2.2. Frequency in interferometry technique

Interferometry systems typically employ two frequencies: narrowband and broadband. Interferometry using narrowband frequencies works at a constant frequency. On the other hand, interferometry with broadband frequencies operates in a frequency range where electromagnetic emissions from lightning can be observed. Broadband frequency outperforms the other because it can record high-resolution electromagnetic emissions, allowing for more accurate monitoring of lightning properties [18].

Most interferometry systems began with narrowband frequencies pioneered by Warwick *et al.* [21], which employed a frequency of 34 MHz with two antennas 80 m apart. The quadrature phase-detection technique identifies the arrival direction's phase difference of arrival (DoA). This interferometry device could determine the position of lightning within certain limits, but it could not eradicate the fringe formed by the electric field. Over the next two years, the system was developed by utilising the same frequency but lowering the antenna distance to 15 m and adding a second baseline perpendicular to the first baseline to calculate the angle of arrival [22]. With this arrangement, the system can estimate the position of lightning in two dimensions, but phase determination remains ambiguous. As a result, multiple baselines are necessary [39].

The research by [23], [44] observed various lightning discharge phenomena in cloud-to-ground (CG) flash, such as dart leader, K-events in the cloud, and attempted leader using radio frequencies with a bandwidth of 6 MHz and a centre frequency of 274 MHz. Even though radio frequencies are susceptible, not all breakdown events can be recorded. To address this, Mazur *et al.* [46] outfitted the interferometry system used by Rhodes *et al.* [45] with a high-speed camera capable of 1000 frames per second. On the other hand, Lojou *et al.* [28] recommends using narrowband interferometry with frequencies close to 100 MHz because this frequency provides better detection results. With a detection range of 300 km, a frequency of 100 MHz produces a reasonably good signal to noise ratio (SNR).

The basic concept of broadband interferometry is the estimation of phase differences in the various frequency components of the Fourier spectrum between a pair of broadband antennas [26], [27], [34], [47] with three main stages: i) extraction of phase differences from electromagnetic pulses in two antennas using discrete Fourier transformation; ii) calculate the cosine angle between the signal coming and the baseline antenna, and iii) derive the azimuth and angular elevation of the radiation source [48]. The researchers preferred interferometry with a broadband frequency rather than a narrowband frequency. The VHF broadband interferometry can describe the physical process during lightning flashes in greater detail [39]. The VHF frequency (30–300 MHz) is common in interferometry techniques. Furthermore, various digital signal processing techniques can improve the quality of input signals, such as that used by [34], which uses a frequency range of 40–350 MHz, making broadband interferometry the preferred method of many researchers.

On the other hand, large frequency ranges demand a substantial quantity of digital storage capacity. To address this, Mardiana and Kawasaki [27] devised a sequential triggering approach in which memory storage was divided into segments that recorded one electrical broadband pulse for one microsecond. When the amplitude of a detected electromagnetic pulse crossed a threshold value, the trigger circuit worked and captured the required waveform, which was then stored in a single storage segment. This approach recorded 2000 segments in a single second, enabling a more comprehensive recording of electromagnetic emission fast-moving pulses at frequencies ranging from 0 to 250 MHz. The location of fast EM radiation from lightning was calculated by extracting phase differences in the frequency range of 0–250 MHz. The system worked at 25–250 MHz frequency using discrete Fourier transformations. The researchers used a high digitation rate of 500 MHz to address the large frequency bandwidth.

A digital-based VHF-broadband interferometry system was developed by placing analogue to digital converter (ADC) and band-pass filter (BPF) amplifiers (10–250 MHz) on the system [49]. The system was known as the VHF broadband-digital interferometer (VHF broadband-DITF). It produced accurate results with an average azimuth difference of less than 1° and an elevation difference of less than 2°. The system

was refined by [50] using the same techniques introduced by [27] to address the limited data storage memory capacity. This technique was then widely used by other researchers, such as [51], who used this technique by dividing the digitiser memory into 4000 segments and recording 2 microseconds in 2009. At the same time, [37] used an interferometry system to record 2000 samples per segment with an entire segment of 4000. On the other hand, [29] established triggering data on a flash-by-flash basis, recording 2 seconds per trigger.

2.3. Denoising technique in interferometry technique

Measuring lightning electromagnetic fields can be challenging due to various sources of noise. These sources include electronic equipment, AC-DC converter equipment with limited resolution due to the signal-to-noise ratio, TV waves, and improper grounding system connections between different sections of the measuring system [52]. In a lightning measuring system, noise or unwanted signals that cannot be controlled might impact some areas of the signal's frequency spectrum [53]. Therefore, a denoising technique is required to eliminate noise from the data while keeping the significant aspects of the studied signal [54].

Broadband interferometry processing methods include the linear fit approach, wavelet transform (WT), and cross-correlation [18]. Shao and Krehbiel [34] interferometry system utilised the linear fit approach to detect the direction of electromagnetic emission sources by integrating the results of measuring phase differences between antenna pairs in an array. The study's primary objective was to look for frequency phase differences. Ushio *et al.* [26] employed a linear fit method slightly different from in their interferometry, employing two orthogonal baselines that allow lightning strikes to be mapped in two dimensions and fitted with trigger mechanisms to permit emission radiation recording.

The cross-correlation approach examines two separate signals to see if they are related, and this approach may also determine the similarity between two separate signal series. In general, adding or multiplying the functions of two signals yields a degree of similarity or correlation. The broadband interferometer system in [27] employed the cross-correlation approach to computing the phase difference of two fast-moving electromagnetic signals. This phase difference is used to compute the magnitude of the incidence angle of the signal source. Compared to the narrowband interferometer system, their study showed that the azimuth direction's mean difference was less than 1° with a standard deviation of 4.5° and the elevation direction's mean difference was less than 2° with a standard deviation of 5.0° [55]. The angle uncertainty was less than 1° when generalised cross-correlation was employed to determine the difference in time of the signal arriving at the two antennas [29]. Puricer *et al.* [43] suggested utilising the cross-correlation approach to increase the performance of interferometry techniques and minimise calculations.

In improving the accuracy, the cross-correlation technique can be combined with other techniques. Alammari *et al.* [56] combined this technique with a WT using the Symlet function, known as the cross-correlation wavelet domain (CCWD), with a resulting error rate of 3.46° . The CCWD method was refined with particle swarm optimisation (PSO). The CCWD technique generated an initial estimate of the location of the lightning, which was then optimised using PSO [57].

The WT is a multiresolution signal processing approach that employs a BPF. This method adjusts or shifts a wave of signals to sort data according to the frequency component required. WT functions include Morlet, Daubechies, Coiflets, Bioorthogonal, Mexican Hat, Myers, Haar, derivative of Gaussian (DOG), and Symlets. The WT has an advantage over other transformation functions in that it allows for simultaneous signal analysis in both spatial and frequency [58]. These two parameters are required for analysing transient signals such as lightning electric field signals [53]. The WT is recommended for spectrum analysis of non-stationary spectra observed in nature rather than the Fourier transform [59]. The latter is better for studying the stationary power spectrum.

Furthermore, due to the wide range of dominant frequencies in the signal, such as lightning, the WT is better suited for analysis requiring independent scale [60]. Lightning's electric field is a non-periodic and transient pulse with an irregular signal waveform, making it difficult to identify its characteristics using conventional transformations such as the Fourier transform [53]. The WT does not "refine" the sharp structure of the analysed signal during the noise removal process, so important signal details are preserved [61].

Three primary parameters are required to evaluate a signal using a WT: the mother wavelet, which represents the signal to be studied; the wavelet function, which translates the mother wavelet; and wavelet thresholding. The signal decomposition procedure creates a daughter wavelet due to the translation of the mother wavelet. The translation outcome will be affected by the number of decomposition levels used at this step. Using five wavelet levels resulted in good noise elimination in the lightning signal [53]. Wavelet thresholding is used to remove noise while keeping the required signal properties.

Studies have found that the Haar discrete wavelet method is an effective way to identify the return stroke (RS) channel in lightning signals [62]. Another research showed that examining the behavior of the RS in the time spectrum and its relationship to its power spectrum can be accomplished by using the DOG function in continuous WT [63]. Furthermore, this research demonstrated that the WT is superior to the Fourier transform's frequency dimension for analyzing lightning characteristics. A separate study demonstrated that utilizing the Myers WT function to eliminate noise from VHF radiation enhances accuracy in incidence angle resolution and

improves dependability in noise reduction, resulting in a clearer depiction of lightning branches [51]. In addition, employing short baseline interferometry and combining the Fourier transformation with Symlet WT functions effectively removes high frequencies exceeding 200 MHz, enabling the system to detect nearby lightning discharges and reveal specific details about the lightning emission [35].

3. INTERFEROMETRY TECHNIQUE ELECTRIC FIELD MEASUREMENT SYSTEM

3.1. Parallel plate antenna

In electromagnetic lightning theory, the lightning channel is assumed to be vertical; thus, its electromagnetic field is also vertical. Therefore, a parallel plate antenna is the most suitable for this condition because its construction is oriented perpendicular to the electric field vector, parallel to or near the surface soil [64]. Another advantage is its ability to determine the location of lightning strikes, particularly lightning within a 10 km radius, simply by measuring the intensity of the electric field [65]. Furthermore, compared to the electric field mill, the parallel plate antenna has a higher time resolution in measuring the electromagnetic field [66]. The distance between the plates remains independent of where it is placed as long as the antenna is grounded [67]. A parallel plate antenna with a buffer circuit is a wideband system that can measure and record lightning electric field waveforms up to 16 MHz [68]. A parallel plate antenna is placed above ground level for lightning E-field measurements, as shown in Figure 3 and the E-field wavelength is much larger than the size of the metal plate.

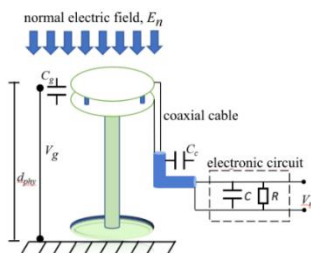


Figure 3. A typical parallel plate antenna equipped with an electronic circuit [64]

The E-field is the force per unit charge for each point in the charge region:

$$E = \frac{F}{Q} = \frac{Q}{4\pi\epsilon_0\epsilon_r r^2} \quad (10)$$

where Q represents charge, r is distance, and ϵ_0 and ϵ_r are absolute and relative permittivity.

The variable $E \epsilon_0 \epsilon_r$ is the flux density, D, which indicates the size of the electric field flowing out of a spherical surface. Based on Gauss's law.

$$\int_s D \cdot ds = Q \quad (11)$$

If the charge is distributed uniformly, the charge density per unit volume is used instead of the closed charge on the surface. Therefore, by integrating over the volume v, Gauss's law in (11) becomes (12):

$$\int_s D \cdot ds = \int \rho \cdot dv \quad (12)$$

In this condition, a charge Q is induced when an electromagnetic field is generated on the antenna plate so that (12) becomes (13):

$$D \cdot S = Q \quad (13)$$

in (10), where $E \epsilon_0 \epsilon_r$ is the flux density D, then the normal electromagnetic field is (14):

$$E_n = \frac{Q}{\epsilon_0 \epsilon_r S} \quad (14)$$

thus, the induced voltage between the parallel plate antenna and the earth, V_g , is (15):

$$V_g = - \int_0^d E_n dx = \frac{Q}{\epsilon_0 \epsilon_r S} \int_0^d (-1) dx = \frac{Qd}{\epsilon_0 \epsilon_r S} \quad (15)$$

substituting (14) to (15) will get the relationship between the voltage between the antenna-earth with a normal electromagnetic field as (16):

$$V_g = E_n \cdot d \quad (16)$$

In (16) shows that the voltage between the parallel plate antenna and the ground is proportional to the normal electromagnetic field on the plate and the antenna's height above the earth's surface—the antenna height d , modified to get the effective height, $d_{\text{effective}}$. The effective height is the distance between the measuring circuit and the antenna connected via a 50Ω coaxial cable.

3.2. Buffer amplifier as an electronic measurement circuit

In order to minimise any distortion of the lightning electric field, the antenna is usually placed far away from the recording equipment. This circumstance necessitates lengthy coaxial cables, which require a matching resistor at the oscilloscope's input to avoid undesired reflections [64]. As a result, a buffer circuit is employed to separate the antenna's high impedance and provide enough power to push the signal from the antenna to the oscilloscope through the coaxial connection. The buffer circuit additionally filters the frequency spectrum of the lightning flash signal without amplifying it [69].

Galván and Fernando [64] pioneered buffers for measuring electrical elements, which other researchers afterwards adopted. The main components of this circuit are an IC component serving as a buffer, an R1C1 component serving as a filter circuit, a $100 \text{ M}\Omega$ -high resistance R_2 serving as a decay time constant regulator, and a matching resistance R_3 serving as a back termination resistor of IC component. The maximum total value of the termination resistor, i.e., R_3 and IC output resistance, is 50Ω . The aim is to equalise the value of the coaxial cable resistance. Given that this circuit is employed in the high-frequency range, matching impedance is required to match the load with the line's characteristic impedance [70], [71]. Figure 4 depicts the design of the electronic measuring circuit.

In the circuit shown in Figure 4, two high-frequency ceramic capacitors, each $0.1 \mu\text{F}$ (C_3 and C_4 in Figure 4), are used to bypass power supply connections and put as near as possible to the buffer IC's power supply ports to provide high-frequency decoupling. To prevent the circuit from damage caused by large currents, a 100Ω resistor was added in line with the power supply pins (R_4 and R_5 in Figure 4). A large ground plane was employed to reduce high-frequency ground drops and stray coupling. This special consideration was paid to the circuit layout design for optimal performance when measuring high frequencies.

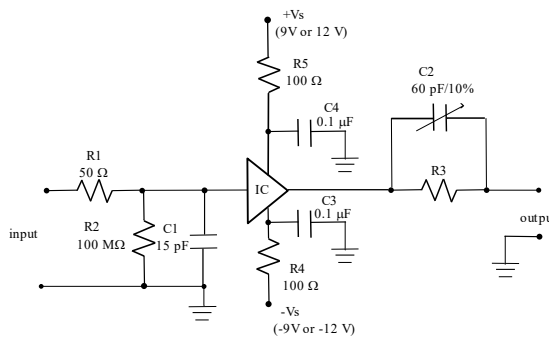


Figure 4. Typical electronic measurement circuit [64]

The IC must be a high-speed buffer with unity gain characteristics and produce a high output current. Using a high-speed buffer enables accurate measurement of the amplitude and rise time of the lightning electric field. Galván and Fernando [64] used ICs from the LH0033 family, while Edirisinghe *et al.* [71] used the OPA633 type (the latest OPA 633KP). The LH0033 is a high-speed input/buffer voltage FET from DC to over 100 MHz frequencies. The LH0033 slews at $1500 \text{ V}/\mu\text{s}$ and exhibits excellent phase linearity up to 20 MHz, making it suitable as a high-impedance input buffer. In comparison, the OPA633 features a bandwidth of 260 MHz with a high slew rate of $2500 \text{ V}/\mu\text{s}$. Both types of ICs can produce high output currents (100 mA), allowing them to drive 50Ω lines.

The capacitor value in the buffer circuit must be as small as possible to keep the total impedance of the circuit from becoming too high, given that the circuit operates at high frequencies. Furthermore, a small

capacitor will offer a suitable decay time constant, 13 ms [64], [71], [72], or 15 ms [69], allowing reasonable-accuracy recording of the electric field signal created by lightning. The capacitor C1 in the fast electric field circuit is 15 pF [64], [71], [72], whereas the capacitor in the slow electric field circuit is 10 nF [72].

4. PARAMETER AFFECTING THE ACCURACY OF INTERFEROMETRY TECHNIQUE

Many researchers have used parallel plate antennas coupled with amplifiers to determine the location or direction of lightning strikes. Based on these studies, the interferometry method appears promising because it has advantages over other methods, such as not requiring a large number of antennas or stations; thus, it is quite economical while providing results with a high degree of accuracy. Previous studies have produced lightning strike/location detection systems with varying accuracy from one study to another. The spatial accuracy rate of interferometry techniques was affected by the “installation error” level and corrected by simple calibration using broadcast waves [73]. The efficiency of each detection method varies according to the type of processing of the observed frequency band. Low- or medium-frequency bands provided long-range detection but limited precision with little detail. In contrast, high frequencies (VHF) or UHF can provide better and more detailed observations [43].

Two significant factors must be considered to improve the performance of a lightning location detection system. They were; i) the automatic extraction of ITF signals derived from lightning events and ii) the noise signal filtering process at the pre-processing stage that must be done carefully; thus, relevant lightning information was not omitted and can be used later [57]. Performance metrics were applied to compare the systems used in one study with those used in other studies to determine other factors affecting the accuracy of previous study results. Table 2 (in Appendix) summarises some performance metrics from previous studies conducted between 2015 and 2021 [29], [39]-[44], [56], [57], [74]-[81].

5. PRELIMINARY RESULTS OF THE PROPOSED ELECTRIC FIELD MEASUREMENT SYSTEM

One of the causes of the phenomenon of gradual changes in the characteristics and intensity of lightning is climate change [82]-[84]. This phenomenon has led to many researchers focusing on observing the characteristics of lightning as their research topic. One crucial characteristic of lightning to be observed is the RS characteristic. The RS is a lightning discharge's most recognizable and powerful component. Climate change may influence thunderstorms' characteristics, potentially affecting lightning's frequency and intensity, including RSs. Therefore, observing the RS characteristic may also lead to the trend of climate change patterns that would affect renewable energy production. Lightning characteristics were observed by observing the changes in lightning's electric field emissions (E-field). These changes were detected using a parallel plate antenna. The block diagram of the configuration of the measurement system used is shown in Figure 5. The Picoscope display was set up in order to capture the changes in E-field emissions, specifically focusing on the RS wave. The Picoscope's configuration as follows, recording time: 1 ms, number of samples: 10 MS, hardware resolution: 12 bit, trigger mode: single, coupling mode: AC, voltage range channel A: +5 V (fast field), voltage range channel B: +2 V (slow field).

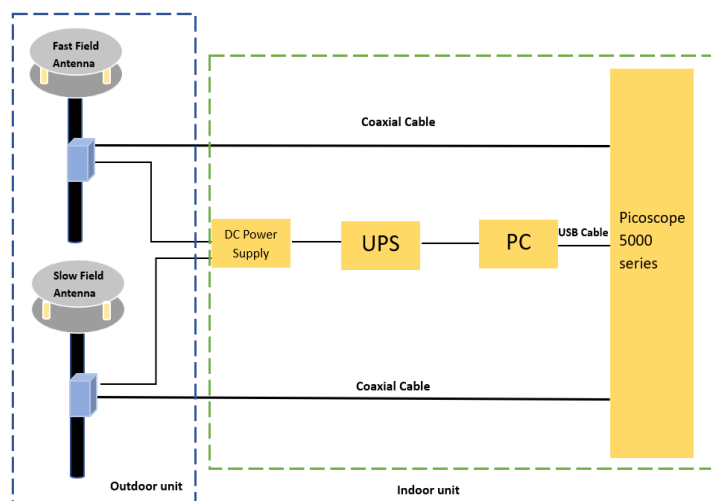


Figure 5. Block diagram of the E-field measurement system

A trigger level for channel A (fast field) was set up at 2 V and 20% pre-trigger time for data captured in December 2022, while for January–February 2023, trigger level and pre-trigger time was set up at 1 V and 30%, respectively. The difference in trigger values aims to determine the measurement system's sensitivity in detecting E-field signal emissions. The smaller the trigger value, the greater the distance between the E-field emission source and measurement station. The intensity of lightning storms in Indonesia generally increases in January and February; hence the potential for lightning storms also increases. Therefore, the trigger value was set to 1 V during those months to test whether the system can detect E-field variations. The captured waves were confirmed with satellite data showing lightning storm activity that coincides with the capture time. Figures 6(a)–(c) shows some of the E-field changes during that time. The highest peak magnitude captured by the system was 7.691 V.

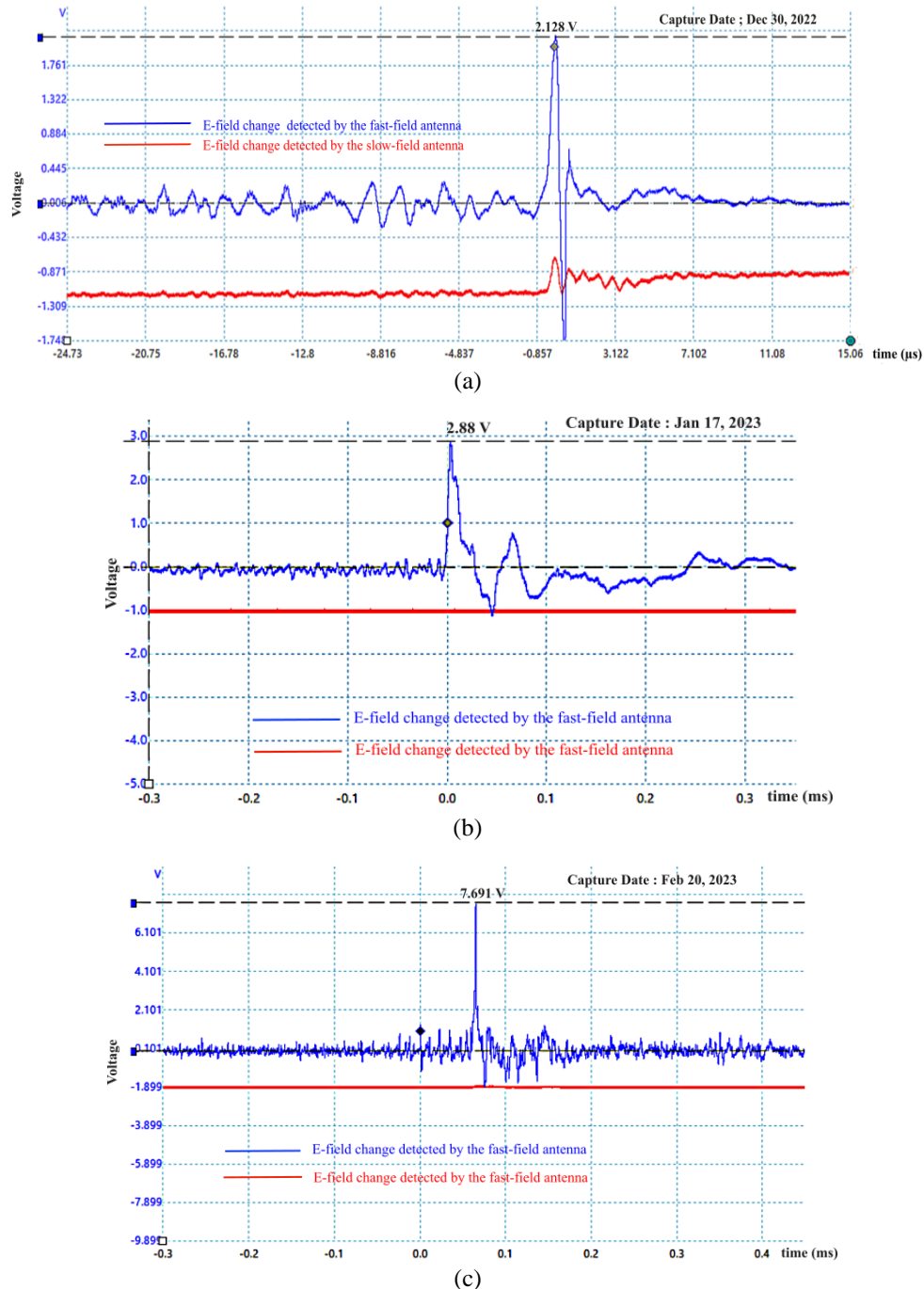


Figure 6. Electric field voltage signal captured on; (a) December 30, 2022, (b) January 17, 2023, and (c) February 20, 2023 with peak voltage magnitude of 2.128 V, 2.88 V, and 7.691 V respectively

6. DISCUSSION

The impacts of climate change and extreme weather events challenged energy production from renewable sources such as wind turbines and photovoltaic systems. These systems need to be designed to withstand weather variability and climate change impacts and be protected from lightning strikes to enhance the sustainability and resilience of renewable energy systems. Monitoring lightning can help keep track of climate change patterns and improve lightning protection system's ability.

Interferometry was a lightning observation and localisation technique with advantages over other lightning detection techniques. It can be operated with only one station, does not need many antennas, and provides reasonably accurate observations. The quality of the received signal influences the accuracy of interferometry. Therefore, the pre-processing stage/signal denoising process becomes crucial because the challenge is producing a clean signal without reducing, obscuring, or even eliminating important parameters of the studied signal.

Another thing that needs to be considered in developing this interferometry technique is the improved capacity of storage media, which is quite large. In addition to sequential triggering techniques, a digital signal oscilloscope or a database management system such as MySQL can relatively overcome memory storage limitations. With the development of digital signal processing technology, recording and displaying real-time lightning signal observation data is possible. However, signal ("signal cleanliness") is the main factor in generating valid data.

The parallel plate antenna is a good choice for detecting or capturing lightning signals since it is built with its construction perpendicular to the vertical electric field vector. This construction makes it possible for the antenna or sensor to accurately measure the lightning's electromagnetic field by capturing it more. The development of this antenna could focus on finding ways to make the parallel plate antenna's dimensions smaller, more portable, and easier to install.

The operational functionality of the measurement system holds paramount significance when measuring the intensity of the electric field in lightning. The signal magnitude is contingent upon the lightning strike's intensity and the distance between the strike and the measuring antenna. Observing changes in the electromagnetic field of lightning over a sufficient period of time will provide insights into the waveform of lightning field emissions, the trend of peak waveform variations, and their relationship with climate change. Typically, the recorded electric field signals captured by the proposed system had a maximum peak magnitude of 7.691 V.

7. CONCLUSION

Lightning activity is typically associated with precipitation events and indicates climate change. Since renewable energy, like wind and solar energy, are influenced by atmospheric phenomena, studies of lightning activity are crucial for their resilience and sustainability. Additionally, lightning protection systems for renewable energy infrastructure must be designed using research on lightning activity. Consequently, lightning detection and localisation systems are essential for investigating lightning field characteristics and locating cloud-to-ground flash lightning, which is dangerous for humans and causes property damage. A decent detection result can be achieved using interferometry without many antennas or spaces. The improvement of interferometry-based lightning detection and localisation systems required the development of signal-processing techniques. In order to enhance system performance, it is also necessary to increase storage capacity and develop suitable storage medium technology. If this is accomplished, real-time monitoring and detecting lightning will be possible. Furthermore, provide sufficient data for lightning intensity analysis to investigate the possibility of future climate change trends and how they relate to the design of climate-resistant renewable energy systems.

APPENDIX

Table 2. The accuracy and parameters of lightning detection systems in previous research (2015-2021)

Ref. No.	Location	Frequency	Baseline	No. of antenna	Pre-processing method and instrumentation	System performance
[40]	Nanjing, China	50–300 MHz	18 m	4 antennas with 2 additional VHF broad band antennas that serve as emitters	TR techniques were applied to determine the location of lightning VHF emissions and mapped the entire lightning process using EMTR-VHF.	EMTR-VHF method performed well, especially for sources with low elevation, with errors less than 1°.

Table 2. The accuracy and parameters of lightning detection systems in previous research (2015-2021)
(continued)

Ref. No.	Location	Frequency	Baseline	No. of antenna	Pre-processing method and instrumentation	System performance
[41]	Guangdong, China	20–300 MHz	16 m for Site A and 15 m for Site B	4 flat circular antennas/site. The distance between the two sites is 8.2 km	Calculation of location accuracy using the measurement method “Theodolite Wind.”	Both stations had high observational accuracy on both sides of the relationship between the two sites. The accuracy rate of the location decreased when the distance of both stations with the radiation source increased, or the height of the radiation source decreased. A 3-D lightning localisation system with two interferometer stations suitable for observing lightning at close range and high elevation angles in small areas
[42]	Colombo, Srilanka	10-80 MHz	10 m	3 flat circular antennas	The direction of the lightning radiation source was calculated by the cross-correlation technique and mapped in 2 D.	The developed system could map lightning development in two spatial dimensions with high time resolution. The results of the interferometer system were verified using a video camera, and the results were consistent.
[43]	Milešovka Hill, Checko	20–60 MHz	6 m	3 antennas	Artificial intercloud pulse generators were applied to test and calibrate the precision of interferometry systems.	System performance would be optimal when the installation location was based on electromagnetic interference measurements in VHF tapes.
[44]	China	It uses two spectrums of signal frequencies, 25-90 MHz and 110-150 MHz	9 m (The positioning of the antenna takes the shape of the letter L)	7 antennas	Using the same system configuration used in the multiple-antenna observation and EMTR processing of lightning VHF radiations [40]. Applying the MUSIC algorithm to the system aims to separate the signal from the noise. The music algorithm was based on parsing the eigenvalues of the covariance matrix.	The location accuracy rate on a MUSIC-VHF system was the same as the EMTR-VHF method (in Gaussian noise) with an SNR=−12 dB value for RMSE< 10, but the music-VHF spatial resolution was better than EMTR-VHF for high SNR. The MUSIC-VHF method performed better than the EMTR-VHF and INTF methods in sidelobe pressing capabilities and withstanding narrowband interference.
[56]	Klebang Beach, Malacca Strait, Melaka, Malaysia	40–80 MHz	15 m	3 antennas	Using a single VHF ITF tested with 3 different processing types: BPF, Kalman filter (KF), and WT.	The system generated a well-estimated source of lightning radiation using wavelet denoising and CCWD with an error of at least 3.460.
[57]	Malaka, Malaysia	NA	15 m	3 antennas	The WT technique was used to process the results of lightning location detection obtained from the ITF system to provide reliable lightning location estimates before being optimised with PSO techniques. Parameters to be aware of in PSO techniques were the maximum and minimum size of “windows” and the number of iterations.	The CCWD-PSO algorithm applied to the ITF technique did not require prior lightning location information. The CCWD-PSO hybrid algorithm could locate the lightning source with a population size of less than 50 and some iterations of less than 500. PSO method excelled in optimisation of lightning location.

Table 2. The accuracy and parameters of lightning detection systems in previous research (2015-2021)
(continued)

Ref. No.	Location	Frequency	Baseline	No. of antenna	Pre-processing method and instrumentation	System performance
[74]	Uchida-Chuo, Ishikawa Prefecture Japan	30–80 MHz	Using 2 baselines; 7.18 m dan 6.55 m	3 antennas were placed, forming a blunt angular triangle of 105.7°. Azimuth and elevation were calculated against the blunt angle	The standard slope deviation of phase difference every two years was used to distinguish VHF pulses were associated with a lightning release. The data recordings were divided into 128 sample windows and were organised into domain frequencies using FFT.	The system could record many VHF pulses associated with lightning release, allowing the perfect mapping of release propagation channels.
[75]	International Space Station, Japan	70–100 MHz	1.62 m	2 antennas	This study used the interferometry technique combined with ionospheric propagation delay measurements, and both were used to determine the direction of arrival from VHF sources.	The system generated location uncertainty of several kilometres at an altitude of 10 km. The approximate position of radiation spatially corresponded to the lightning position captured with the lightning and sprite imager (LSI).
[76]	Jiangsu, China	50–300 MHz	18 m	4 antennas	The interferometry technique combined with high-speed video (HSV) was placed as far as 3 km from the antenna site.	The results obtained from interferometry techniques were consistent with the visual results of HSV.
[77]	Shandong, China	140–300 MHz	8 m	4 antennas	LMI was based on TDOA short baseline technology. The lightning electric field changes were processed using cross-correlation time delay algorithms based on correlation and parabolic interpolation algorithms.	LMI could effectively reproduce lightning development in the clouds for rocket-triggering and natural lightning flashes. LMI results were consistent with results from high-speed cameras (optical seeding)
[78]	Durham, North Carolina- USA	100 kHz– 55 MHz	52 m	3 aluminium plate antennas	Before VHF signals were processed dispersively, digital high pass filter filters were applied to raw data to limit the signal frequency band to 20–55 MHz.	For signals with an SNR of 10 dB, the angular uncertainty was about 0.1° at a source elevation of 45°. Standard deviations (elevation and uncertainty of azimuth angles) were 0.17° and 0.26°, respectively.
[79]	Durham, North Carolina- USA	100–200 MHz	52 m	3 antennas	Interferometric and imaging proceedings using cross-correlation algorithms were also used by Stock <i>et al.</i> [29].	The system could image in a synchronous needle that correlated with negative leaders and bidirectional leaders during intra-cloud lightning flashes with much higher spatial resolution than previous systems with the maximum frequency of 60 MHz.
[80]	Leshan, China	48.2 MHz	Using two baselines, $d_1=5 \lambda/2$ and $d_2=9 \lambda/2$.	1 transmitter antenna and 5 receiving antennas	Determination of the location of lightning using interferometry techniques that were treated as radar. This radar system transmitted electromagnetic pulses and received echoes reflected by lightning channels. Lightning localisation results verified. Search results of lightning detection networks operating in the VLF range indicate the feasibility of using VHF radar for lightning mapping.	The accuracy of point locations in 3D still needs to be improved further. Verification results with the VLF system showed that the VHF radar interferometry system had similar latitude and longitude from the source, but that was not the case with altitude.

Table 2. The accuracy and parameters of lightning detection systems in previous research (2015-2021)
(continued)

Ref.No.	Location	Frequency	Baseline	No. of antenna	Pre-processing method and instrumentation	System performance
[81]	Córdoba, Argentina	1.6 kHz – 2.5 MHz for fast channel	10–60 km	10 antennas	This imaging algorithm was similar to the VHF interferometry algorithm presented in [39]. The difference lay in how to project the location. Stock and Krehbiel [39] project the location into a 2D cosine plane, while [81] imaging algorithms project it in Cartesian 3D volumes. In imaging algorithms, the location was determined by maximising the total correlation between a pair of stations.	Imaging algorithms could find more sources than interferometric-TOA hybrid algorithms and produce more complete lightning maps. However, the height of the lightning source obtained from the imaging algorithm was more dispersive, which indicates that the error in determining the height of the lightning source was more significant than the previous algorithm.

REFERENCES

- [1] G. Sarma and A. Zabaniotou, "Understanding vulnerabilities of renewable energy systems for building their resilience to climate change hazards: key concepts and assessment approaches," *Renewable Energy and Environmental Sustainability*, vol. 6, p. 35, Oct. 2021, doi: 10.1051/rees/2021035.
- [2] P. Ravestein, G. van der Schrier, R. Haarsma, R. Scheele, and M. van den Broek, "Vulnerability of European intermittent renewable energy supply to climate change and climate variability," *Renewable and Sustainable Energy Reviews*, vol. 97, pp. 497–508, Dec. 2018, doi: 10.1016/j.rser.2018.08.057.
- [3] H. W. Cutforth and D. Judiesch, "Long-term changes to incoming solar energy on the Canadian Prairie," *Agricultural and Forest Meteorology*, vol. 145, no. 3, pp. 167–175, Aug. 2007, doi: 10.1016/j.agrmet.2007.04.011.
- [4] V. Penmetsa and K. E. Holbert, "Climate change effects on solar, wind and hydro power generation," in *2019 North American Power Symposium (NAPS)*, Oct. 2019, pp. 1–6, doi: 10.1109/NAPS46351.2019.9000213.
- [5] N. Reeve and R. Toumi, "Lightning activity as an indicator of climate change," *Quarterly Journal of the Royal Meteorological Society*, vol. 125, no. 555, pp. 893–903, Apr. 1999, doi: 10.1002/qj.49712555507.
- [6] E. R. Williams, "Lightning and climate: a review," *Atmospheric Research*, vol. 76, no. 1–4, pp. 272–287, Jul. 2005, doi: 10.1016/j.atmosres.2004.11.014.
- [7] C. Price, "Thunderstorms, lightning and climate change," in *Lightning: Principles, Instruments and Applications*, H. D. Betz, U. Schumann, and P. Laroche, Eds., Dordrecht: Springer Netherlands, 2008, pp. 521–535, doi: 10.1007/978-1-4020-9079-0_24.
- [8] Z. Yijun, M. Ming, and L. Weitao, "Review on climate characteristics of lightning activity," *Acta Meteorologica Sinica*, vol. 24, no. 1, pp. 137–149, 2010.
- [9] O. Pinto, "Lightning and climate: a review," in *2013 International Symposium on Lightning Protection (XII SIPDA)*, Oct. 2013, pp. 402–404, doi: 10.1109/SIPDA.2013.6729250.
- [10] D. Romps, J. Seeley, D. Vollaro, and J. Molinari, "Climate change. Projected increase in lightning strikes in the United States due to global warming," *Science (New York, N.Y.)*, vol. 346, pp. 851–4, Nov. 2014, doi: 10.1126/science.1259100.
- [11] G. Paliaga, C. Donadio, M. Bernardi, and F. Faccini, "High-resolution lightning detection and possible relationship with rainfall events over the central mediterranean area," *Remote Sensing*, vol. 11, no. 13, no. 13, Jan. 2019, doi: 10.3390/rs11131601.
- [12] O. P. Jr and I. R. C. A. Pinto, "Lightning changes in response to global warming in Rio de Janeiro, Brazil," *American Journal of Climate Change*, vol. 9, no. 3, no. 3, Aug. 2020, doi: 10.4236/ajcc.2020.93017.
- [13] R. H. Holzworth, J. B. Brundell, M. P. McCarthy, A. R. Jacobson, C. J. Rodger, and T. S. Anderson, "Lightning in the Arctic," *Geophysical Research Letters*, vol. 48, no. 7, 2021, doi: 10.1029/2020GL091366.
- [14] IRENA, *Global energy transformation: A roadmap to 2050 (2019 edition)*. International Renewable Energy Agency, 2019. [Online]. Available: <https://www.irena.org/publications/2019/Apr/Global-energy-transformation-A-roadmap-to-2050-2019Edition>. (Accessed: Feb. 12, 2023).
- [15] K. Solaun and E. Cerdá, "Climate change impacts on renewable energy generation. A review of quantitative projections," *Renewable and Sustainable Energy Reviews*, vol. 116, p. 109415, Dec. 2019, doi: 10.1016/j.rser.2019.109415.
- [16] M. Adrian, E. P. Purnomo, A. Enrici, and T. Khairunnisa, "Energy transition towards renewable energy in Indonesia," *Heritage and Sustainable Development*, vol. 5, no. 1, no. 1, May 2023, doi: 10.37868/hsd.v5i1.108.
- [17] K. L. Cummins and M. J. Murphy, "An overview of lightning locating systems: history, techniques, and data uses, with an in-depth look at the U.S. NLDN," *IEEE Transactions on Electromagnetic Compatibility*, vol. 51, no. 3, pp. 499–518, Aug. 2009, doi: 10.1109/TEMC.2009.2023450.
- [18] A. Alammari *et al.*, "Lightning mapping: techniques, challenges, and opportunities," *IEEE Access*, vol. 8, pp. 190064–190082, 2020, doi: 10.1109/ACCESS.2020.3031810.
- [19] P. Krehbiel, X.-M. Shao, R. Thomas, C. Rhodes, and C. Hayenga, "VHF radio interferometry of lightning," *International Astronomical Union Colloquium*, vol. 19, p. 372, Jan. 1991, doi: 10.1017/S025292110001366X.
- [20] C. O. Hayenga, "Positions and movement of VHF lightning sources determined with microsecond resolution by interferometry," University of Colorado at Boulder, May 1979.
- [21] J. W. Warwick, C. O. Hayenga, and J. W. Brosnahan, "Interferometric directions of lightning sources at 34 MHz," *Journal of Geophysical Research: Oceans*, vol. 84, no. C5, pp. 2457–2468, 1979, doi: 10.1029/JC084iC05p02457.
- [22] C. O. Hayenga and J. W. Warwick, "Two-dimensional interferometric positions of VHF lightning sources," *Journal of Geophysical Research: Oceans*, vol. 86, no. C8, pp. 7451–7462, 1981, doi: 10.1029/JC086iC08p07451.
- [23] P. Richard and G. Auffray, "VHF-UHF interferometric measurements, applications to lightning discharge mapping," *Radio Science*, vol. 20, no. 2, pp. 171–192, 1985, doi: 10.1029/RS020i002p00171.

[24] C. Rhodes and P. R. Krehbiel, "Location and analysis of lightning VHF radio sources using interferometry," in *10th Annual International Symposium on Geoscience and Remote Sensing*, May 1990, pp. 1893–1893, doi: 10.1109/IGARSS.1990.688893.

[25] X. M. Shao, D. N. Holden, and C. T. Rhodes, "Broad band radio interferometry for lightning observations," *Geophysical Research Letters*, vol. 23, no. 15, pp. 1917–1920, 1996, doi: 10.1029/96GL00474.

[26] T. Ushio, Z.-I. Kawasaki, Y. Ohta, and K. Matsuura, "Broad band interferometric measurement of rocket triggered lightning in Japan," *Geophysical Research Letters*, vol. 24, no. 22, pp. 2769–2772, 1997, doi: 10.1029/97GL02953.

[27] R. Mardiana and Z. Kawasaki, "Broadband radio interferometer utilizing a sequential triggering technique for locating fast-moving electromagnetic sources emitted from lightning," *IEEE Transactions on Instrumentation and Measurement*, vol. 49, no. 2, pp. 376–381, Apr. 2000, doi: 10.1109/19.843081.

[28] J.-Y. Lojou, M. J. Murphy, R. L. Holle, and N. W. S. Demetriades, "Nowcasting of thunderstorms using VHF measurements," in *Lightning: Principles, Instruments and Applications: Review of Modern Lightning Research*, H. D. Betz, U. Schumann, and P. Laroche, Eds., Dordrecht: Springer Netherlands, 2009, pp. 253–270, doi: 10.1007/978-1-4020-9079-0_11.

[29] M. G. Stock *et al.*, "Continuous broadband digital interferometry of lightning using a generalized cross-correlation algorithm," *Journal of Geophysical Research: Atmospheres*, vol. 119, no. 6, pp. 3134–3165, 2014, doi: 10.1002/2013JD020217.

[30] V. Cooray, *An Introduction to Lightning*. Dordrecht: Springer Netherlands, 2015, doi: 10.1007/978-94-017-8938-7.

[31] M. Akita, M. Stock, Z. Kawasaki, P. Krehbiel, W. Rison, and M. Stanley, "Data processing procedure using distribution of slopes of phase differences for broadband VHF interferometer," *Journal of Geophysical Research: Atmospheres*, vol. 119, no. 10, pp. 6085–6104, 2014, doi: 10.1002/2013JD020378.

[32] X. M. Shao, P. R. Krehbiel, R. J. Thomas, and W. Rison, "Radio interferometric observations of cloud-to-ground lightning phenomena in Florida," *Journal of Geophysical Research: Atmospheres*, vol. 100, no. D2, pp. 2749–2783, 1995, doi: 10.1029/94JD01943.

[33] R. Ismail and Z. A. Baharudin, "A review on basic principle of lightning location in multi-station system and the ability of single-station measurement," in *2016 IEEE International Conference on Power and Energy (PECon)*, Nov. 2016, pp. 62–67, doi: 10.1109/PECON.2016.7951534.

[34] X. M. Shao and P. R. Krehbiel, "The spatial and temporal development of intracloud lightning," *Journal of Geophysical Research: Atmospheres*, vol. 101, no. D21, pp. 26641–26668, 1996, doi: 10.1029/96JD01803.

[35] D. Cao, X. Qie, S. Duan, J. Yang, and Y. Xuan, "Observations of VHF source radiated by lightning using short baseline technology," in *2010 Asia-Pacific International Symposium on Electromagnetic Compatibility*, Apr. 2010, pp. 1162–1165, doi: 10.1109/APEMC.2010.5475866.

[36] M. Akita and Z. Kawasaki, "VHF broadband interferometer observations and micro-structure of lightning discharge," in *2010 Asia-Pacific International Symposium on Electromagnetic Compatibility*, 2010, pp. 1134–1137, doi: 10.1109/APEMC.2010.5475746.

[37] Z. Sun, X. Qie, M. Liu, D. Cao, and D. Wang, "Lightning VHF radiation location system based on short-baseline TDOA technique—Validation in rocket-triggered lightning," *Atmospheric Research*, vol. 129–130, pp. 58–66, Jul. 2013, doi: 10.1016/j.atmosres.2012.11.010.

[38] Y. Nakamura, L. S. M. Elbaghdady, T. Wu, T. Ushio, and Z. Kawasaki, "Development and initial observations of a long-period VHF broadband digital interferometer," *2014 International Conference on Lightning Protection (ICLP)*, Shanghai, China, 2014, pp. 1583–1586, doi: 10.1109/ICLP.2014.6973382.

[39] M. Stock and P. Krehbiel, "Multiple baseline lightning interferometry - Improving the detection of low amplitude VHF sources," *2014 International Conference on Lightning Protection (ICLP)*, Shanghai, China, 2014, pp. 293–300, doi: 10.1109/ICLP.2014.6973139.

[40] T. Wang, S. Qiu, L.-H. Shi, and Y. Li, "Broadband VHF localization of lightning radiation sources by EMTR," *IEEE transactions on electromagnetic compatibility*, vol. 59, no. 6, pp. 1949–1957, 2017, doi: 10.1109/TEMC.2017.2651142.

[41] H. Liu, S. Qiu, and W. Dong, "The three-dimensional locating of VHF broadband lightning interferometers," *Atmosphere*, vol. 9, no. 8, no. 8, Aug. 2018, doi: 10.3390/atmos9080317.

[42] R. Abeywardhana, U. Sonnadar, S. Abegunawardana, M. Fernando, and V. Cooray, "Lightning localization based on VHF broadband interferometer developed in Sri Lanka," in *2018 34th International Conference on Lightning Protection (ICLP)*, Rzeszow, Poland, 2018, pp. 1–5, doi: 10.1109/ICLP.2018.8503396.

[43] P. Puricic, P. Kovac, and J. Mikes, "New accuracy testing of the lightning VHF interferometer by an artificial intercloud pulse generator," *IEEE Transactions on Electromagnetic Compatibility*, vol. 62, no. 5, pp. 2128–2136, 2020, doi: 10.1109/TEMC.2019.2947706.

[44] T. Wang, L. Shi, S. Qiu, Z. Sun, and Y. Duan, "Continuous broadband lightning VHF mapping array using MUSIC algorithm," *Atmospheric Research*, vol. 231, p. 104647, Jan. 2020, doi: 10.1016/j.atmosres.2019.104647.

[45] C. T. Rhodes, X. M. Shao, P. R. Krehbiel, R. J. Thomas, and C. O. Hayenga, "Observations of lightning phenomena using radio interferometry," *Journal of Geophysical Research: Atmospheres*, vol. 99, no. D6, pp. 13059–13082, 1994, doi: 10.1029/94JD00318.

[46] V. Mazur, P. R. Krehbiel, and X.-M. Shao, "Correlated high-speed video and radio interferometric observations of a cloud-to-ground lightning flash," *Journal of Geophysical Research: Atmospheres*, vol. 100, no. D12, pp. 25731–25753, 1995, doi: 10.1029/95JD02364.

[47] T. Morimoto, Z. Kawasaki, and T. Ushio, "An operational VHF broadband digital interferometer and thunderstorm observation," *Lightning Research Group of Osaka University (LRG-Ou)*, vol. 124, no. 12, pp. 1232–1238, 2004.

[48] T. Ushio, Z.-I. Kawasaki, M. Akita, S. Yoshida, T. Morimoto, and Y. Nakamura, "A VHF broadband interferometer for lightning observation," in *2011 XXXth URSI General Assembly and Scientific Symposium*, Aug. 2011, pp. 1–4, doi: 10.1109/URSIGASS.2011.6050771.

[49] T. Morimoto, A. Hirata, Z. Kawasaki, T. Ushio, A. Matsumoto, and L. Ho, "An operational VHF broadband digital interferometer for lightning monitoring," *Ieej Transactions on Fundamentals and Materials*, vol. 124, no. 12, pp. 1232–1238, Jan. 2004, doi: 10.1541/ieejfms.124.1232.

[50] T. Morimoto and Z. Kawasaki, "VHF broadband digital interferometer," *IEEJ Transactions on Electrical and Electronic Engineering*, vol. 1, no. 2, pp. 140–144, 2006, doi: 10.1002/tee.20030.

[51] S. Qiu, B.-H. Zhou, L.-H. Shi, W.-S. Dong, Y.-J. Zhang, and T.-C. Gao, "An improved method for broadband interferometric lightning location using wavelet transforms," *Journal of Geophysical Research: Atmospheres*, vol. 114, no. D18, 2009, doi: 10.1029/2008JD011655.

[52] C. Cortés, F. Santamaría, F. Roman, F. Rachidi, and C. Gomes, "Analysis of wavelet based denoising methods applied to measured lightning electric fields," in *2010 30th International Conference on Lightning Protection (ICLP)*, Sep. 2010, pp. 1–6, doi: 10.1109/ICLP.2010.7845950.

[53] F. Santamaría, C. Cortés, and F. Roman, "Noise reduction of measured lightning electric fields signals using the wavelet transform," *X International Symposium on Lightning Protection*, Nov. 2009, pp. 525–530.

[54] X. Ma, C. Zhou, and I. J. Kemp, "Automated wavelet selection and thresholding for PD detection," *IEEE Electrical Insulation Magazine*, vol. 18, no. 2, pp. 37–45, Mar. 2002, doi: 10.1109/57.995398.

[55] Z. Kawasaki, R. Mardianan, and T. Ushio, "Broadband and narrowband RF interferometers for lightning observations," *Geophysical Research Letters*, vol. 27, no. 19, pp. 3189–3192, 2000, doi: 10.1029/1999GL011058.

[56] A. Alammari *et al.*, "Kalman filter and wavelet cross-correlation for VHF broadband interferometer lightning mapping," *Applied Sciences*, vol. 10, no. 12, Art. no. 12, Jan. 2020, doi: 10.3390/app10124238.

[57] A. Alammari, A. A. Alkahtani, M. R. Ahmad, A. Aljanad, F. Noman, and Z. Kawasaki, "Cross-correlation wavelet-domain-based particle swarm optimization for lightning mapping," *Applied Sciences*, vol. 11, no. 18, no. 18, Jan. 2021, doi: 10.3390/app11188634.

[58] N. M. Astaf'eva, "Wavelet analysis: basic theory and some applications," *Physics-uspekhi*, vol. 39, no. 11, p. 1085, Nov. 1996, doi: 10.1070/PU1996v03n11ABEH000177.

[59] I. Daubechies, "The wavelet transform, time-frequency localization and signal analysis," *IEEE Transactions on Information Theory*, vol. 36, no. 5, pp. 961–1005, Sep. 1990, doi: 10.1109/18.57199.

[60] C. Torrence and G. P. Compo, "A practical guide to wavelet analysis," *Bulletin of the American Meteorological Society*, vol. 79, no. 1, pp. 61–78, Jan. 1998, doi: 10.1175/1520-0477(1998)079<0061:APGTWA>2.0.CO;2.

[61] J. Ramirez-Niño, S. Rivera-Castañeda, V. R. Garcia-Colon, and V. M. Castaño, "Analysis of partial electrical discharges in insulating materials through the wavelet transform," *Computational Materials Science*, vol. 9, no. 3, pp. 379–388, Jan. 1998, doi: 10.1016/S0927-0256(97)00165-1.

[62] K. Sheshyekani, M. Hazrati, P. Sattari, S. H. H. Sadeghi, and R. Moini, "Real-time detection of lightning electromagnetic field data: a wavelet approach," in *2006 17th International Zurich Symposium on Electromagnetic Compatibility*, Feb. 2006, pp. 413–415, doi: 10.1109/EMCZUR.2006.214959.

[63] F. J. Miranda, "Wavelet analysis of lightning return stroke," *Journal of Atmospheric and Solar-Terrestrial Physics*, vol. 70, no. 11, pp. 1401–1407, Aug. 2008, doi: 10.1016/j.jastp.2008.04.008.

[64] A. Galván and M. Fernando, "Operative characteristics of a parallel-plate antenna to measure vertical electric fields from lightning flashes," 2000.

[65] M. A. B. Sidik *et al.*, "Lightning monitoring system for sustainable energy supply: a review," *Renewable and Sustainable Energy Reviews*, vol. 48, pp. 710–725, 2015, doi: 10.1016/j.rser.2015.04.045.

[66] V. Cooray, Ed., *Lightning electromagnetics*, 1st edition. London: The Institution of Engineering and Technology, 2012.

[67] A. Santa-Acosta, L. M. Morales-Garcia, and H. E. Rojas-Cubides, "Practical method to evaluate the effects of the sensor and the environment on the measurement of lightning-generated electric field signatures," *Engineering Journal*, vol. 25, no. 8, pp. 137–152, Aug. 2021, doi: 10.4186/ej.2021.25.8.137.

[68] M. R. Ahmad, "Interaction of Lightning flashes with wireless communication networks: special attention to narrow bipolar pulses," Uppsala University, Sweden, 2014. [Online]. Available: <http://urn.kb.se/resolve?urn=urn:nbn:se:uu:diva-233673>. (Accessed: Feb. 09, 2023).

[69] M. R. M. Esa, M. R. Ahmad, and V. Cooray, "Wavelet analysis of the first electric field pulse of lightning flashes in Sweden," *Atmospheric Research*, vol. 138, pp. 253–267, Mar. 2014, doi: 10.1016/j.atmosres.2013.11.019.

[70] M. Haziq, "Initial electric field changes of lightning flashes in tropical thunderstorms," Mater Thesis, FKEKK, University Teknikal Malaysia Melaka, Melaka-Malaysia, 2018.

[71] C. M. Edirisinghe, I. M. K. Fernando, and D. U. J. Sonnadara, "Construction of a high speed buffer amplifier to measure lightning generated vertical electric fields," in *Proceedings of the Technical Sessions*, Sri Lanka: Institute of Physics – Sri Lanka, 2001, pp. 21–29.

[72] M. H. M. Sabri *et al.*, "Initial electric field changes of lightning flashes in tropical thunderstorms and their relationship to the lightning initiation mechanism," *Atmospheric Research*, vol. 226, pp. 138–151, Sep. 2019, doi: 10.1016/j.atmosres.2019.04.013.

[73] Y. Nakamura, T. Morimoto, T. Ushio, and Z.-I. Kawasaki, "An error estimate of the VHF broadband digital interferometer," *IEEJ Transactions on Fundamentals and Materials*, vol. 129, no. 8, pp. 525–530, 2009, doi: 10.1541/ieejfms.129.525.

[74] L. Samy, Y. Nakamura, A. Allam, T. Ushio, and Z. Kawasaki, "Ten minutes continuous recording lightning using broadband VHF interferometer," *Advances in Space Research*, vol. 56, no. 10, pp. 2218–2234, Nov. 2015, doi: 10.1016/j.asr.2015.07.038.

[75] H. Kikuchi *et al.*, "Direction-of-arrival estimation of VHF signals recorded on the international space station and simultaneous observations of optical lightning," *IEEE Transactions on Geoscience and Remote Sensing*, vol. 54, no. 7, pp. 3868–3877, 2016, doi: 10.1109/TGRS.2016.2529658.

[76] Y. Li, S. Qiu, L. Shi, Z. Huang, T. Wang, and Y. Duan, "Three-dimensional reconstruction of cloud-to-ground lightning using high-speed video and VHF broadband interferometer," *Journal of Geophysical Research: Atmospheres*, vol. 122, no. 24, pp. 13,420–13,435, Dec. 2017, doi: 10.1002/2017JD027214.

[77] Z. Sun, X. Qie, M. Liu, R. Jiang, and H. Zhang, "Lightning mapping interferometer observations on lightning discharge," *2017 XXXIIInd General Assembly and Scientific Symposium of the International Union of Radio Science (URSI GASS)*, Montreal, QC, Canada, 2017, pp. 1–4, doi: 10.23919/URSIGASS.2017.8105179.

[78] F. Lyu, S. A. Cummer, Z. Qin, and M. Chen, "Lightning initiation processes imaged with very high frequency broadband interferometry," *Journal of Geophysical Research: Atmospheres*, vol. 124, no. 6, pp. 2994–3004, 2019, doi: 10.1029/2018JD029817.

[79] Y. Pu and S. A. Cummer, "Needles and lightning leader dynamics imaged with 100–200 MHz broadband VHF interferometry," *Geophysical Research Letters*, vol. 46, no. 22, pp. 13556–13563, 2019, doi: 10.1029/2019GL085635.

[80] W. Yin *et al.*, "Lightning detection and imaging based on VHF radar interferometry," *Remote Sensing*, vol. 13, no. 11, p. 2065, May 2021, doi: 10.3390/rs13112065.

[81] Y. Zhu, M. Stock, and P. Bitzer, "A new approach to map lightning channels based on low-frequency interferometry," *Atmospheric Research*, vol. 247, p. 105139, Jan. 2021, doi: 10.1016/j.atmosres.2020.105139.

[82] D. L. Finney, R. M. Doherty, O. Wild, D. S. Stevenson, I. A. MacKenzie, and A. M. Blyth, "A projected decrease in lightning under climate change," *Nature Climate Change*, vol. 8, no. 3, pp. 210–213, Mar. 2018, doi: 10.1038/s41558-018-0072-6.

[83] E. Williams, A. Guha, R. Boldi, H. Christian, and D. Buechler, "Global lightning activity and the hiatus in global warming," *Journal of Atmospheric and Solar-Terrestrial Physics*, vol. 189, pp. 27–34, Aug. 2019, doi: 10.1016/j.jastp.2019.03.011.

[84] K. Qie, X. Qie, and W. Tian, "Increasing trend of lightning activity in the South Asia region," *Science Bulletin*, vol. 66, no. 1, pp. 78–84, Jan. 2021, doi: 10.1016/j.scib.2020.08.033.

BIOGRAPHIES OF AUTHORS



Wiwin A. Oktaviani is an Assistant Professor at the Department of Electrical Engineering, Faculty of Engineering, Universitas Muhammadiyah Palembang, Indonesia where she has been a faculty member since 2012. From 2000-2011 she became a lecturer at Department of Electrical Engineering, Faculty of Engineering, Universitas Lampung before she joined her currently department. She received a bachelor's degree in electrical engineering from Sriwijaya University in 1997 and a master's degree in the same field from University of Manchester Institute of Science and Technology (UMIST) in 1999. Currently, she is pursuing her doctoral studies with a research focus on lightning characteristics and lightning location detection systems. She can be contacted at email: win.oktaviani1973@gmail.com.



Muhammad Abu Bakar Sidik, S.T., M.Eng., Ph.D., IPU is a Lecturer in the Department of Electrical Engineering, Faculty of Engineering, Universitas Sriwijaya. He received a bachelor's in electrical engineering from Universitas Sriwijaya in 1995. After graduating, he worked for a company that developed telecommunications networks for Sumatra Island for two years and seven months. Then in March 1999, he was accepted as a lecturer candidate at the Department of Electrical Engineering, Universitas Sriwijaya. In 2003 he received a master's degree in high-voltage insulators, and in 2008 received a doctorate in lightning protection from Universiti Teknologi Malaysia. From 2010 to 2020, he was a visiting lecturer and researcher at Institut Voltan dan Arus Tinggi (IVAT) Universiti Teknologi Malaysia. His research on lightning includes characterisation, location determination systems, real-time monitoring systems, and protection systems. He can be contacted at email: abubakar@unsri.ac.id.



Mohd Riduan Ahmad received the degree (Hons.) in computer system and communication engineering from the Universiti Putra Malaysia, in 2003, the M.Eng. degree with a specialisation in cross-layer design of MAC protocols for multi-in multi-out-based wireless sensor network from the University of Wollongong, Australia, in 2008, and the Ph.D. degree with a specialisation in atmospheric discharges from Uppsala University, Sweden, in 2014. From 2015 to 2016, he was with the MIT, USA, where he focused on the understanding and characterisation of microwave radiation emitted by lightning flashes. He is currently the manager of Centre of Technology for Disaster Risk Reduction (CDR), Universiti Teknikal Malaysia Melaka (UTeM). He is also an Associate Professor with the Faculty of Electronics and Computer Technology and Engineering, UTeM. He can be contacted at email: riduan@utem.edu.my.



Muhammad Irfan Jambak was born in Palembang, Indonesia. He obtained his bachelor of engineering (B.Sc.) in electrical engineering from Universitas Sriwijaya in 1996. From 1995 to 1998, he worked at PT. Lapi Elpatsindo in his last position as Engineering Manager. After that, he obtained his M.Eng. with a research focus on grounding resistance measurement and Ph.D. research focus on switching over-voltages of six-phase transmission lines in Electrical Engineering from Universiti Teknologi Malaysia in 2001 and 2009 respectively. Currently he is a senior lecturer in the Department of Electrical Engineering, Faculty of Engineering Universitas Sriwijaya, South Sumatera, Indonesia. His research interest included external and internal lightning protection systems, grounding systems, and automation systems including the development, repair, and modification of high-voltage equipment and test facility. He can be contacted at email: irfjambak@unsri.ac.id.